

**BIMODAL CRATERS ON VESTA: IMPACTS ON SLOPES STUDIED BY GEOLOGICAL**

**INVESTIGATIONS.** K. Krohn<sup>1</sup>, R. Jaumann<sup>1,2</sup>, D. Elbeshhausen<sup>3</sup>, T. Kneissl<sup>2</sup>, R. Wagner<sup>1</sup>, K. Stephan<sup>1</sup>, K. Otto<sup>1</sup>, K.D. Matz<sup>1</sup>, F. Preusker<sup>1</sup>, T. Roatsch<sup>1</sup>, N. Schmedemann<sup>2</sup>, C.A. Raymond<sup>4</sup>, C.T. Russell<sup>5</sup>

<sup>1</sup>Institute of Planetary Research, German Aerospace Center (DLR), Berlin, Germany, <sup>2</sup>Freie Universität Berlin, Inst. of Geosciences, Planetology and Remote Sensing, <sup>3</sup>Museum für Naturkunde, Leibniz Institute for Research on Evolution and Biodiversity, Berlin, Germany, <sup>4</sup>Jet Propulsion Laboratory, California Institute of Technology, Pasadena, USA, <sup>5</sup>UCLA, Institute of Geophysics, Los Angeles, USA (Katrin.Krohn@dlr.de)

**Introduction:**

Vesta exhibits a significant number of craters impacting on sloping surfaces [1,2] with an unusual asymmetrical shape. Six different types of unusual craters can be identified on Vesta. The formation of this bimodal craters and is constrained by numerical simulations [3] and age determination of the ejecta in order to distinguish between primary deposition and secondary mass wasting.

**Data and Methods:** For the analysis of the bimodal crater distribution, their mineralogy and ejecta distribution, Dawn Framing Camera data (FC) [4] data as well as the HAMO digital terrain models (DTM) [5] were used. Low Altitude Mapping Orbit (LAMO) with resolutions of 20 m/px are the basis for geological mapping of bimodal craters.

**Types of bimodal craters:**

*Type A:* Craters reveal a relatively steep slope of about 24° to 28° on the uphill side and a shallower one of about 13° to 16° on the downhill side [1]. The craters show an asymmetrical shape with a semi-circular sharp rim on the uphill side and an undefined smooth rim on the downhill side [1,2]. They reveal narrow crater floors cut by a clear border that separates the rims. The uphill inner crater wall shows mass wasting material. Little ejecta is only found over the uphill rim, while ejecta on the downhill side are diffusely distributed over the crater and crater rim area (Fig. 1A) [1,2].

*Type B:* This crater type is characterized by an oblique elongated shape (Fig. 1B). The uphill rim coalesces with the slope whereas the downhill rim is less elevated than type A. The crater floor is wider than type A shows. A relatively straight line between the crater flanks and mass wasting features is observable. The uphill slope average is about 23° to 31° and the downhill slope average is about 7° to 8°. Type B shows the same ejecta distribution as type A [2].

*Type C:* Type C craters show a sharp uphill rim and a less distinctive smooth downhill rim. Ejecta is found all over the rim and covers the crater rim on more than one spot [2]. Mass wasting material and boulders are

observable on the crater walls (Fig. 1C). The crater floor is bowl-shaped and the crater walls have nearly the same slope angle of about 16° [2].

*Type D:* Those craters show a V-shaped crater form with one extended wall (1D). Mass wasting material occurs on the crater flanks. The ejecta is mostly distributed over the downhill rim, but little ejecta is also found over the uphill rim [2].

*Type E:* Type E craters show a lateral elongated form (1E). The uphill slope is about 32° and the downhill slope is about 7° [2]. They show a relatively straight cut between the flanks. The craters have a smooth downhill rim and a sharp uphill rim. Ejecta is mainly found over the downhill rim [2].

*Type F:* A special type of a bimodal crater is shown in crater Eusebia (lat 42.2°S, long 204.5°E). A sharp uphill rim and a smooth downhill rim are observable (1F) [2]. The downhill rim has no distinct border, it passes into the slope. Mass wasting material from the crater flanks are observable. Two scarps in the lower third are broken up the crater walls and reaches semicircular from the crater rims into the middle of the crater [2]. The uphill slope is about 26° and the downhill slope is about 18° [2].

For more geological and geomorphological details see [7].

**Results:** Type A, B and E show similarities in morphology, a sharp crater rim uphill and a smooth one downhill as well as ejecta on the downhill rim and only thin ejecta over the uphill rim. Type C and D show more than one part of the crater rim smoothed and a surrounding ejecta.

We performed crater size frequency measurements to compare surrounding surface, ejecta deposits and crater interiors. Thus the ages of the crater interiors and the ejecta are similar indicating the deposits to be formed directly by the impact and not influenced by subsequently mass wasting processes [1].

Three-dimensional numerical simulations have been performed to study the formation process of the unusual craters [2,3]. The results showed that

- the slope prevents the deposition of ejected material in uphill direction and results in a larger accumulation of ejecta in the crater or even downhill outside of the crater [2,3].

downhill-directed crater collapse results in slumping of uphill-material and products the sharp uphill rim [2,3]. Thus mass accumulation downhill is a mixture of ejected material and material of the initial slope [1].

### Conclusions:

We analyzed the topographic conditions around the different craters and were able to correlate each type of unusual craters with a specific target relief [2,3]. We found that:

- Similar ages of surface, ejecta deposits and crater interiors indicates a formations by the impact

- the formation of the bimodal craters is controlled by topographic conditions and by the steepness of the slopes [2,3],
- craters on high slope angles show a one-sided ejecta distribution [2],
- craters on lower slope angles are surrounded by the ejecta [2].

**References:** [1] Jaumann et al. (2012) *Science*, 336, 687-690. [2] Krohn et al. (2013) *PSS*, submitted. [3] Elbeshausen et al. (2013) *LPSC*, this session #1903. [4] Sierks et al. (2011) *Space Science Rev.* 163, 263-327; [5] Preusker et al. (2012) *LPSC XLIII*, #2012. [6] Kneissl et al. (2011) *Planet. Space Sci.*, 59, 11-12. [7] Kneissl et al. (2013) *LPSC*, this session.

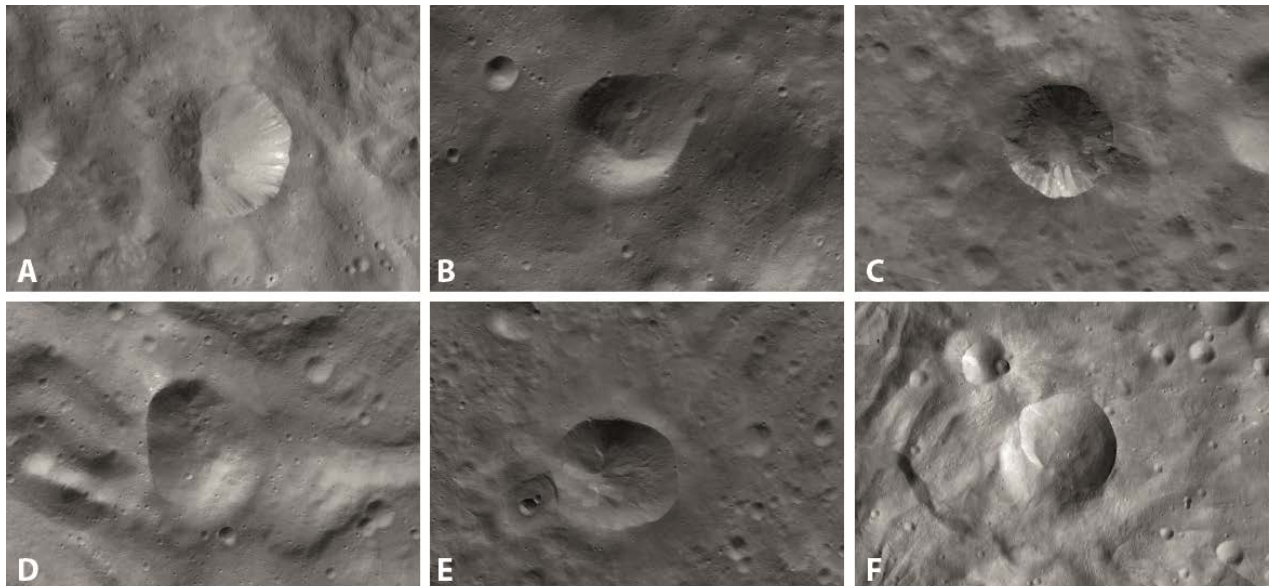


Fig. 1: (A) Type A crater Helena (lat 41.4°S, long 122.5°E); (B) Type B: Oblique elongated craters. LAMO FC image of an unnamed crater at ~lat 6°S, long 299°E. (C) Type C: Rubria (lat 7.4°S, long 18.4°E); (D) Type D: V-shaped crater Oppia (lat 8°S, long 309°E); (E) Lateral elongated unnamed crater of Type E (~ lat 50°S, long 266°E); (F) Type F: LAMO FC image of Eusebia crater (lat 42.2°S, long 204.5°E)